Draft version March 4, 2016
Preprint typeset using LaTeX style emulateapj v. 5/2/11

arXiv:1603.00998v1 [astro-ph.HE] 3 Mar 2016

THE LIKELY *FERMI* DETECTION OF THE SUPERNOVA REMNANT SN 1006

Yi Xing[1], Zhongxiang Wang[1], Xiao Zhang[2], & Yang Chen[2,3]

Draft version March 4, 2016

ABSTRACT

We report the likely detection of γ-ray emission from the northeast shell region of the historical supernova remnant (SNR) SN 1006. Having analyzed 7 years of *Fermi* LAT Pass 8 data for the region of SN 1006, we found a GeV gamma-ray source detected with $\sim 4\sigma$ significance. Both the position and spectrum of the source match those of HESS J1504−418 respectively, which is TeV emission from SN 1006. Considering the source as the GeV γ-ray counterpart to SN 1006, the broadband spectral energy distribution is found to be approximately consistent with the leptonic scenario that has been proposed for the TeV emission from the SNR. Our result has likely confirmed the previous study of the SNRs with TeV shell-like morphology: SN 1006 is one of them sharing very similar peak luminosity and spectral shape.

Subject headings: acceleration of particles — gamma rays: ISM — ISM: individual objects (SN 1006) — ISM: supernova remnants

1. INTRODUCTION

As one of the few supernova remnants (SNRs) that were historically recorded by people from different countries or continents (Stephenson & Green 2002; Stephenson 2010), SN 1006 is of great interest and has been extensively studied at multiple energy bands. It is located far away from the Galactic plane, with a Galactic latitude of $\sim 14^{\circ}.5$, in a relatively low ambient-density ($\sim 0.085\,\mathrm{cm}^{-3}$; e.g., Katsuda et al. 2009) environment. The long-term proper motion measurements of the shock front at optical narrow band, combined with the expanding velocity, implies a distance of $\sim$2.2 kpc for the SNR (Winkler et al. 2003). Multiwavelength emission from SN 1006 shows that the remnant has a diameter of $30'$(or 19 pc at 2.2 kpc), with two main lobes located at northeast (NE) and southwest (SW) parts of the SNR's disk-like region. While the interior of the SNR is dominated by thermal emission (e.g., Uchida et al. 2013), the shell is dominated by synchrotron emission which is bright in radio (Reynolds & Gilmore 1986) and hard X-ray (Rothenflug et al. 2004; Winkler et al. 2014) bands.

SNRs are considered to be the main sites in the Milky Way for producing cosmic rays with energies up to a few 10^{15} eV. Charged particles are accelerated in their shock fronts due to the diffusive shock acceleration mechanism (e.g., Blandford & Eichler 1987). As for SN 1006, in addition to hard X-rays that indicate high-energy electrons accelerated to 100 TeV in the shock front (Koyama et al. 1995), very high energy (VHE; > 100 GeV) emission was also detected with the High Energy Stereoscopic System (HESS). The two HESS sources J1504−418 and J1502−421 correspond to the NE and SW shell regions respectively (Acero et al. 2010), with the former approximately 50% brighter than the latter. Given these, GeV γ-ray emission from SN 1006 has been searched in observations with the Large Area Telescope (LAT) onboard Fermi Gamma-ray Space Telescope (Fermi). Using 3.5 and 6 years of *Fermi* LAT data, only upper limits have been obtained by Araya & Frutos (2012) and Acero et al. (2015a), respectively. Combining the TeV spectrum with the GeV upper limits, a leptonic scenario, in which γ-ray photons arise from the inverse Compton (IC) scattering process, is favored for the γ-ray emission (Acero et al. 2010; Araya & Frutos 2012; Acero et al. 2015a).

The *Fermi* upper limits already tightly constrain the models typically considered for young SNRs (e.g., Cas A: Acero et al. 2010, Araya & Cui 2010; Tycho: Giordano et al. 2012) or for SNRs having a TeV shell-like morphology (Acero et al. 2015a). Evidence for the interaction with a HI cloud in the SW limb region of SN 1006 has been reported by Miceli et al. (2014). With the release of the best *Fermi* LAT dataset (Pass 8 data) in early 2015 and the accumulation of 7 years data, detailed analysis of the γ-ray emission from SN 1006 is thus warranted. In this paper we report our analysis of the *Fermi* LAT data of the SN 1006 region and the likely detection of γ-ray emission in 0.15–300 GeV energy range from the NE region of the SNR.

2. DATA ANALYSIS AND RESULTS

2.1. *Fermi LAT Data*

LAT is a γ-ray imaging instrument that scans the whole sky every three hours and is basically conducting long-term γ-ray observations of GeV sources (Atwood et al. 2009). For this analysis we selected *Fermi* LAT Pass 8 events in the energy range from 150 MeV to 300 GeV centered at the SIMBAD position of SN 1006, which is $(\alpha_{J2000}, \delta_{J2000}) = (15^{\mathrm{h}}02^{\mathrm{m}}22^{\mathrm{s}}.1, -42^{\circ}05'49''.0)$, obtained by Wright & Otrupcek (1990). The events below 150 MeV were excluded to reduce the effects of the Galactic background and the relatively large uncertainties of the instrument response function of the LAT in low energy range. The time period of the LAT data is from 2008-08-04 15:43:36 (UTC) to 2015-09-24

[1] Key Laboratory for Research in Galaxies and Cosmology, Shanghai Astronomical Observatory, Chinese Academy of Sciences, 80 Nandan Road, Shanghai 200030, China
[2] Department Astronomy, Nanjing University, 163 Xianlin Avenue, Nanjing 210023, China
[3] Key Laboratory of Modern Astronomy and Astrophysics, Nanjing University, Ministry of Education, Nanjing 210023, China

00:03:16 (UTC). Following the recommendations of the LAT team[4], we included those events with zenith angles less than 90 degrees, which prevents the Earth's limb contamination, and excluded the events with quality flags of 'bad'.

2.2. *Source Detection*

We included all sources within 20 degrees centered at the position of SN 1006 in the *Fermi* LAT 4-year catalog (Acero et al. 2015b) to make the source model. The spectral forms of these sources are provided in the catalog. Spectral parameters of the sources within 5 degrees from SN 1006 were set as free parameters, and the other parameters were fixed at their catalog values. The background Galactic and extragalactic diffuse emission were also added in the source model with the spectral model gll_iem_v06.fits and the file iso_P8R2_SOURCE_V6_v06.txt, respectively, used. The normalizations of the diffuse components were set as free parameters.

We first performed standard binned likelihood analysis to the LAT data in the >1 GeV band using the LAT science tool *gtlike* in the science tools software package `v10r0p5`. The Instrument Response Functions (IRFs) of P8R2_SOURCE_V6 were used. Test Statistic (TS) maps obtained in this higher energy range would likely be better resolved in a possibly crowded region and source positions be better determined as well. With the fitted source model, we calculated the binned TS map (using *gttsmap* in the *Fermi* software package) of a $2^{\circ} \times 2^{\circ}$ region centered at SN 1006. All sources in the source model were considered and removed. The obtained residual TS map of the source region is shown in the top panel of Figure 1. Excess emission in the SN 1006 region was detected with a maximum TS value of ∼25. The TS value at a given position is a measurement of the fit improvement for including a source, and is approximately the square of the detection significance of the source (Abdo et al. 2010). Therefore, the excess was detected with 5σ significance. We noted that no catalog sources are within the square region, but there is an additional source in the top left corner of the TS map.

We investigated if the nearby additional source might contaminate the detection of the excess emission in the SN 1006 region. We ran *gtfindsrc* in the LAT software package, and determined its position: $(\alpha_{J2000}, \delta_{J2000}) = (227.^{\circ}0, -41.^{\circ}2)$ with 1σ nominal uncertainty of $0.^{\circ}2$. Adding the nearby source in the source model as a point source with power-law emission at its best-fit position, we re-performed the binned likelihood analysis. The TS map with this nearby source considered in the source model is shown in the bottom panel of Figure 1. Now with the nearby source totally removed, the maximum TS value for the excess emission in the SN 1006 region was ∼22, still significant. In the following analysis the nearby source was considered in the source model. For the confirmed excess source, we determined its position, which is $(\alpha_{J2000}, \delta_{J2000}) = (225.^{\circ}9, -41.^{\circ}8)$ with 1σ nominal uncertainty of $0.^{\circ}1$. The VHE source HESS J1504−418 (Acero et al. 2010, marked in Figure 1) is $0.^{\circ}08$ from the best-fit position and within the 1σ error circle.

[4] http://fermi.gsfc.nasa.gov/ssc/data/analysis/scitools/

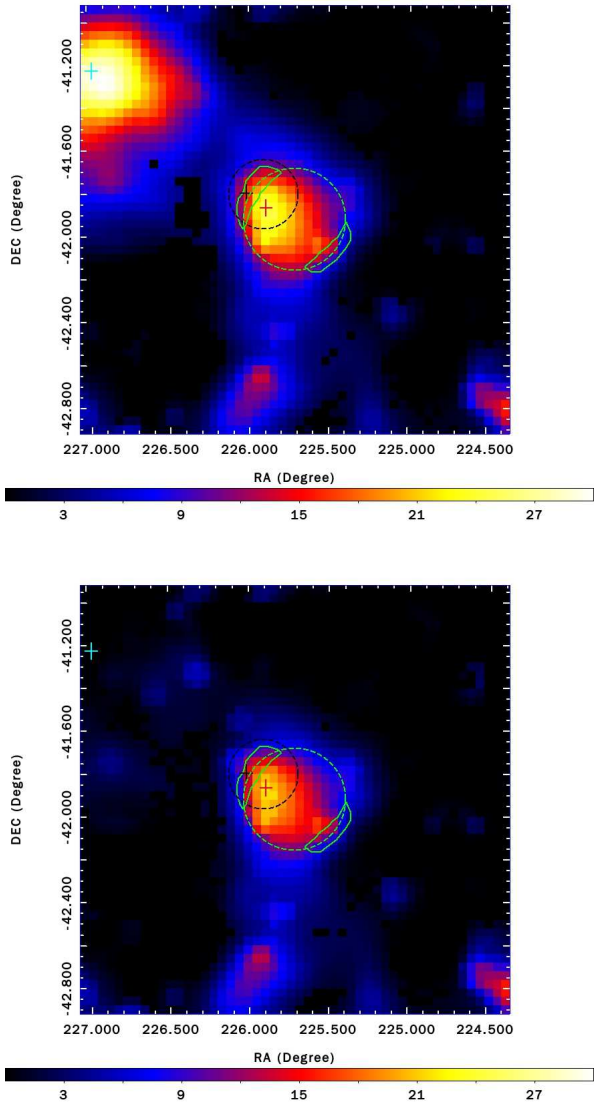

FIG. 1.— TS maps of the $2^{\circ} \times 2^{\circ}$ region centered at the X-ray center of SN 1006 in the 1–300 GeV band, with the green dashed circle indicating the X-ray region of SN 1006 and the green contours indicating the 2.0–7.2 keV X-ray intensity measurements of the NE and SW limbs of SN 1006 (at a level of 19 counts s^{-1}; obtained from the XMM-Newton map rebinned to the $\sim 0.^{\circ}04$ pixel^{-1} scale). The image scale of the maps is $0.^{\circ}04$ pixel^{-1}. All catalog sources were considered and removed. The non-catalog source detected in the top left corner (the *top* panel, indicated by a cyan cross) was removed in the *bottom* panel. The dark and red crosses mark the positions of HESS J1504−418 and QSO J1504−4152, respectively. The dark dashed circle marks the 2σ error circle of the best-fit position obtained for the excess emission.

We then investigated whether the confirmed excess source is point-like or extended. Using both point-source and uniform disk models with power-law spectra at the best-fit position, we performed likelihood analysis to the data in 1–300 GeV energy range. The radius for the uniform disk was set in a range of $0.^{\circ}1$–$0.^{\circ}5$ with a step of $0.^{\circ}1$. The spectral parameters of the sources within 5 degrees from SN 1006 were set as free parameters, and all other parameters in the source model were fixed at their catalog values. No significant extended emission was detected. The TS_{ext} values, calculated from

$TS_{disk} - TS_{point}$ (see, e.g., Lande et al. 2012), were smaller than 0. We included the excess source as a point source in the source model with power-law emission and performed likelihood analysis in 0.15–300 GeV band. The photon index $\Gamma = 1.9 \pm 0.3$ and the photon flux $F_{0.15-300} = 7 \pm 2 \times 10^{-10}$ photons $s^{-1}\,cm^{-2}$ were obtained, with a TS value of 15.

2.3. *Variability Analysis*

In addition to the VHE source HESS J1504−418, there is an another known source located in the 2σ error circle of the best-fit position, that is the quasar QSO J1504−4152 (Winkler & Long 1997). Its position is marked in Figure 1. Given that active galactic nuclei (AGN) are the dominant source class detected by *Fermi* LAT (Acero et al. 2015b), we thus searched for long-term variability for the purpose of checking any possible association between QSO J1504−4152 and the excess source. We calculated the variability index TS_{var} for the point source in SN 1006 region with 87 time bins (each bin constructed from 30-day data) in the energy range of 0.15–300 GeV, following the procedure introduced in Nolan et al. (2012). If the flux is constant, TS_{var} would be distributed as χ^2 with 86 degrees of freedom. Variable sources would thus be identified with TS_{var} larger than 119.4 (at a 99% confidence level in the χ^2 distribution; see Nolan et al. 2012). The computed TS_{var} for the source is 48.9, corresponding to a <1% confidence level for a variable source. The value indicates that there was no signifiant long-term variability observed in the γ-ray source.

2.4. *Spectral Analysis*

Considering the excess emission at the SN 1006 region as a point source at the best-fit position, we extracted its γ-ray spectrum by performing likelihood analysis to the LAT data in 5 evenly divided energy bands in logarithm from 0.15–300 GeV. The excess emission was modelled with a power law in each energy band. The fluxes obtained in this way are not dependent on the emission model assumed for a source, providing a good description for the γ-ray emission of the source. In the extraction, the spectral normalizations of the sources within 5 degrees from the central position of SN 1006 were set as free parameters, while all the other parameters of the sources were fixed at the values obtained from the above maximum likelihood analysis. The obtained spectrum is plotted in Figure 2, where we kept the data points with TS greater than 9 (corresponding to the detection significance of 3σ), and derived 95% flux upper limits otherwise. The fluxes (or flux upper limits) and TS values are provided in Table 1. We also estimated the systematic uncertainties for the spectral data points due to the Galactic diffuse emission model, by repeating the likelihood analysis in each energy band with the normalization of the diffuse component artificially fixed to the ±6% deviation from the best-fit value (see e.g., Abdo et al. 2009, 2010a). The uncertainties estimated in this way are provided in Table 1, which have been considered together with the statistic ones in Figure 2.

3. DISCUSSION AND SUMMARY

Having analyzed 7 years of *Fermi* LAT Pass 8 data, we found excess γ-ray emission at the SN 1006 region.

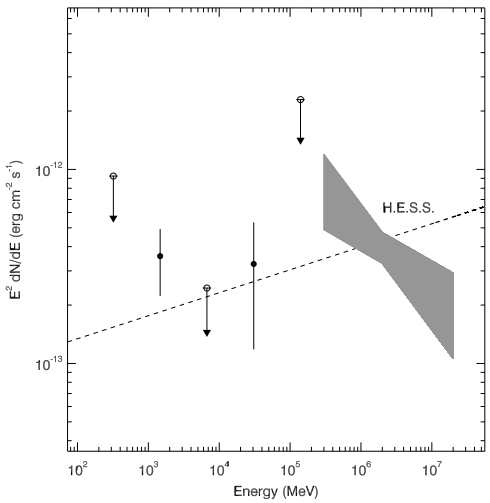

FIG. 2.— *Fermi*-LAT γ-ray spectrum of the excess source at the best-fit position in the SN 1006 region. The 0.15–300 GeV power-law fit to the source is shown as the dashed line. The grey area marks the power-low spectrum for the NE region of SN 1006, obtained with HESS.

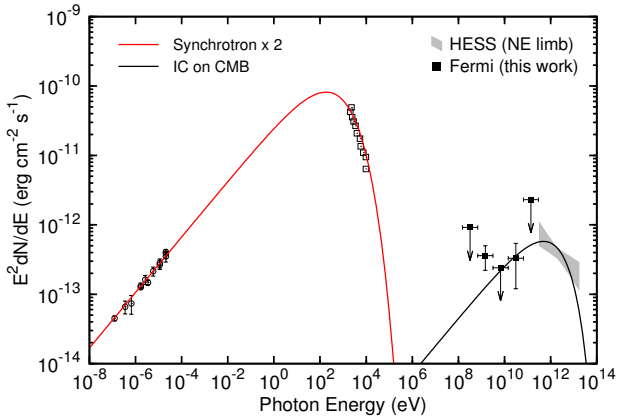

FIG. 3.— Leptonic model fit to the broadband SED of SN 1006. Radio (Allen et al. 2001), Suzaku X-ray (Bamba et al. 2008), HESS (Acero et al. 2010) data are included. The solid curve is the model spectra when $\alpha_e = 2.2$.

As shown in Figure 1 and 2, both the position and spectrum (i.e., the high-energy data point at 30 GeV; see Table 1) match those of the TeV emission from the NE shell region of SN 1006 (see Acero et al. 2010 for details). The detected excess emission may well be the GeV counterpart to SN 1006 that has been previously searched (Araya & Frutos 2012; Acero et al. 2015a). We tested to repeat the analysis in Acero et al. (2015a), where 6 years of P7REP data were used, and obtained the same non-detection result as theirs. Then as we changed to repeat our above analysis using Pass 8 data in the same 6 years time period, the >1 GeV excess emission was detected with TS≃ 20. Therefore our detection of the source should be due to the overall sensitivity improvement in the Pass 8 data.

3.1. *Model Fitting*

Considering the *Fermi* source as the GeV counterpart and combining its spectrum with the HESS TeV one, we checked if a leptonic model that has been

proposed (see Acero et al. 2010; Araya & Frutos 2012; Acero et al. 2015a) could decribe the broadband spectrum of SN 1006. We employed a simple one-zone stationary model, in which the synchrotron and IC emission originates from the same population of electrons with a power-law form plus an exponential cutoff. Given the radio spectral index of ∼0.6 (e.g., Allen et al. 2001), the electron spectral index was set to $\alpha_{\rm e} = 2.2$. To fit the data, for which we have included radio (Allen et al. 2001), X-ray (Bamba et al. 2008), and GeV and TeV γ-ray, the required parameters were found to be: the cutoff energy $E_{\rm cut,e} \approx 17$ TeV, the total electron energy $W_{\rm e}(> 1{\rm GeV}) \approx 1.6 \times 10^{47}\,{\rm erg}$, and the magnetic field strength $B_{\rm SNR} \approx 24\ \mu$G. These parameter values are compatible with those considered in the previous leptonic models (see Araya & Frutos 2012; Acero et al. 2015a). The broadband spectral energy distribution (SED) and the model spectrum are shown in Figure 3, where because the radio and X-ray data were emission from the whole remnant, the synchrotron flux was multiplied by a factor of 2 in our calculation assuming a symmetry between the NE and SW parts for simplicity. Not surprisingly as indicated by the previous studies, the leptonic model generally can describe the broadband data. The observed flux at 1.5 GeV is higher than the model flux, but within the 2σ uncertainty.

3.2. *Summary*

Analysis of the lastest *Fermi* LAT Pass 8 data for the SN 1006 region results in the detection of a source at a $\sim 4\sigma$ significance level in 0.15–300 GeV. The spectrum of the excess emission can be described by a $\Gamma = 1.9$ power law (the dashed line in Figure 2), which can be connected to the HESS spectrum. Both the quasar QSO J1504−4152 (Winkler & Long 1997) and the VHE source HESS J1504−418 (Acero et al. 2010) are within the 2σ error circle of the best-fit position of the source. We searched for variability in the source, but no significant variations were found. In addition the spectral index of 1.9 does not favor the association to AGN since AGN generally have soft power-law spectra with photon indices up to ∼3.0 in the LAT γ-ray energy range (Ackermann et al. 2015). All of these indicate the source is more likely the GeV counterpart to SN 1006.

The combined *Fermi* LAT and HESS spectrum can be described by a leptonic model with reasonable parameters, although the data point at 1.5 GeV is slightly higher than our model spectrum. The discrepancy may suggest that a more complicated model, e.g., multi-emission zones, would be needed in order to better fit the broadband SED. On the other hand, we note that the index $\Gamma = 1.9 \pm 0.3$ is compatible with those of the other 4 (RX J1713.7−3946, RX J0852.0−4622, RCW 86, and HESS J1731−347; $\Gamma \sim 1.5$) TeV shell SNRs summarized by Acero et al. (2015a). This similarity may provide additional evidence for supporting the γ-ray excess emission as the counterpart to the SNR. At the source distance of 2.2 kpc, the 0.15–300 GeV luminosity is 1×10^{33} erg s^{-1}, estimated from the best-fit model. The luminosity value is consistent with the general emissional property for the currently *Fermi* detected SNRs: young SNRs (with ages no larger than a few thousands of years) have γ-ray luminosities of $\sim 10^{33}$–$10^{34}\,{\rm erg\,s^{-1}}$, while middle-aged, dynamically evolved SNRs are two orders of magnitude brighter due to their interaction with nearby molecular clouds (see, e.g., Xing et al. 2015 and references therein).

TABLE 1
Fermi LAT flux measurements of the source in the region of SN 1006

E (GeV)	Band (GeV)	$E^2dN(E)/dE$ (10^{-13} erg cm^{-2} s^{-1})	TS
0.32	0.15–0.69	9.2	2
1.47	0.69–3.14	3.6±1.3±0.4	10
6.71	3.14–14.35	2.4	1
30.68	14.35–65.60	3.3±2.1±0.0	10
140.29	65.60–300.00	23	3

Note: fluxes with uncertainties are given in energy bins with $> 3\sigma$ detection significance, and fluxes without uncertainties are the 95% upper limits. The first and second uncertainties are statistic and systematic ones, respectively.

Finally, Miceli et al. (2014) have reported that the SW limb of SN 1006 is interacting with an atomic cloud, and predicted a 3–30 GeV flux of $5\times10^{-13}\,{\rm erg\,cm^{-2}\,s^{-1}}$ based on their hadronic model proposed to explain the TeV emission. The flux is reached with the current *Fermi* LAT data (see Figure 2). However in our analysis, we did not see any significant sources in the SW region of SN 1006 (see Figure 1). A simple estimation for its flux can be used by scaling the NE flux with the ratio between the HESS SW and NE fluxes (0.67; Acero et al. 2010), which gives 1.5–$3.4\times10^{-13}\,{\rm erg\,cm^{-2}\,s^{-1}}$ and 0.8–$3.6\times10^{-13}\,{\rm erg\,cm^{-2}\,s^{-1}}$ at 1.5 and 30 GeV (Table 1), respectively. With the *Fermi* LAT observation time increasing for the source region, it can be expected that the SW GeV emission would likely be detected in the near future. The detection will help confirm our result presented here in this work.

ACKNOWLEDGEMENTS

This research made use of the High Performance Computing Resource in the Core Facility for Advanced Research Computing at Shanghai Astronomical Observatory. The research was supported by the Shanghai Natural Science Foundation for Youth (13ZR1464400), the National Natural Science Foundation of China for Youth (11403075), the National Natural Science Foundation of China (11373055), and the Strategic Priority Research Program "The Emergence of Cosmological Structures" of the Chinese Academy of Sciences (Grant No. XDB09000000). Z.W. acknowledges the support by the CAS/SAFEA International Partnership Program for Creative Research Teams. Y.C. and X.Z. acknowledge the support of NSFC grant 11233001 and 973 Program grant 2015CB857100.

REFERENCES

Abdo, A. A., Ackermann, M., Ajello, M., et al. 2009, ApJ, 706, L1
—. 2010a, ApJ, 718, 348
Abdo, A. A., Ackermann, M., Ajello, M., et al. 2010, ApJS, 188, 405
Abdo, A. A., Ajello, M., Allafort, A., et al. 2013, ApJS, 208, 17
Acero, F., Lemoine-Goumard, M., Renaud, M., et al. 2015a, A&A, 580, A74
Acero, F., Aharonian, F., Akhperjanian, A. G., et al. 2010, A&A, 516, A62
Acero, F., Ackermann, M., Ajello, M., et al. 2015b, ApJS, 218, 23

Ackermann, M., Ajello, M., Atwood, W. B., et al. 2015, ApJ, 810, 14
Allen, G. E., Petre, R., & Gotthelf, E. V. 2001, ApJ, 558, 739
Araya, M., & Cui, W. 2010, ApJ, 720, 20
Araya, M., & Frutos, F. 2012, MNRAS, 425, 2810
Atwood, W. B., Abdo, A. A., Ackermann, M., et al. 2009, ApJ, 697, 1071
Bamba, A., Fukazawa, Y., Hiraga, et al. 2008, PASJ, 60, S153
Blandford, R., & Eichler, D. 1987, Phys. Rep., 154, 1
Giordano, F., Naumann-Godo, M., Ballet, J., et al. 2012, ApJ, 744, L2
Katsuda, S., Petre, R., Long, K. S., et al. 2009, ApJ, 692, L105
Koyama, K., Petre, R., Gotthelf, E. V., et al. 1995, Nature, 378, 255
Lande, J., Ackermann, M., Allafort, A., et al. 2012, ApJ, 756, 5
Miceli, M., Acero, F., Dubner, G., et al. 2014, ApJ, 782, L33
Nolan, P. L., Abdo, A. A., Ackermann, M., et al. 2012, ApJS, 199, 31
Reynolds, S. P., & Gilmore, D. M. 1986, AJ, 92, 1138
Rothenflug, R., Ballet, J., Dubner, G., et al. 2004, A&A, 425, 121
Stephenson, F. R. 2010, Astronomy and Geophysics, 51, 27
Stephenson, F. R., & Green, D. A. 2002, Historical supernovae and their remnants, by F. Richard Stephenson and David A. Green. International series in astronomy and astrophysics, vol. 5. Oxford: Clarendon Press, 2002, ISBN 0198507666, 5
Uchida, H., Yamaguchi, H., & Koyama, K. 2013, ApJ, 771, 56
Winkler, P. F., & Long, K. S. 1997, ApJ, 486, L137
Winkler, P. F., Gupta, G., & Long, K. S. 2003, ApJ, 585, 324
Winkler, P. F., Williams, B. J., Reynolds, S. P., et al. 2014, ApJ, 781, 65
Wright, A., & Otrupcek, R. 1990, in PKS Catalog (1990), 0
Xing, Y., Wang, Z., Zhang, X., & Chen, Y. 2015, ApJ, 805, 19